



H Bergsaker et al.

## First results from the $^{10}\text{Be}$ marker experiment in JET with ITER-like wall

Preprint of Paper to be submitted for publication in  
Nuclear Fusion Letter



This work has been carried out within the framework of the EUROfusion Consortium and has received funding from the Euratom research and training programme 2014-2018 under grant agreement No 633053. The views and opinions expressed herein do not necessarily reflect those of the European Commission.

This document is intended for publication in the open literature. It is made available on the clear understanding that it may not be further circulated and extracts or references may not be published prior to publication of the original when applicable, or without the consent of the Publications Officer, EUROfusion Programme Management Unit, Culham Science Centre, Abingdon, Oxon, OX14 3DB, UK or e-mail Publications.Officer@euro-fusion.org

Enquiries about Copyright and reproduction should be addressed to the Publications Officer, EUROfusion Programme Management Unit, Culham Science Centre, Abingdon, Oxon, OX14 3DB, UK or e-mail Publications.Officer@euro-fusion.org

The contents of this preprint and all other EUROfusion Preprints, Reports and Conference Papers are available to view online free at <http://www.euro-fusionscipub.org>. This site has full search facilities and e-mail alert options. In the JET specific papers the diagrams contained within the PDFs on this site are hyperlinked

# First results from the $^{10}\text{Be}$ Marker Experiment in JET with ITER-Like Wall

H. Bergsaker<sup>1</sup>, G. Possnert<sup>2</sup>, I. Bykov<sup>1</sup>, K. Heinola<sup>3</sup>, P. Petersson<sup>1</sup>, J. Miettunen<sup>4</sup>,  
A. Widdowson<sup>7</sup>, V. Riccardo<sup>7</sup>, I. Nunes<sup>7</sup>, M. Stamp<sup>7</sup>, S. Brezinsek<sup>8</sup>, M. Groth<sup>4</sup>,  
T. Kurki-Suonio<sup>4</sup>, J. Likonen<sup>5</sup>, J.P. Coad<sup>5</sup>, D. Borodin<sup>8</sup>, A. Kirschner<sup>8</sup>,  
K. Schmid<sup>6</sup>, K. Krieger<sup>6</sup> and JET EFDA contributors\*

*JET Joint Undertaking, Culham Science Centre, OX14 3DB, Abingdon, UK*

<sup>1</sup>*Division of Fusion Plasma Physics, Association EURATOM-VR,  
Royal Institute of Technology KTH, Sweden*

<sup>2</sup>*Tandem Laboratory, Association EURATOM-VR, Uppsala Universitet, Box 256,  
Uppsala 75105, Sweden*

<sup>3</sup>*Department of Physics, University of Helsinki, P.O. Box 64, 00560 Helsinki,  
Association EURATOM-TEKES, Finland*

<sup>4</sup>*Aalto University, Association EURATOM-TEKES, 00076 Aalto, Finland*

<sup>5</sup>*Association EURATOM-TEKES, VTT, PO Box 1000, 02044 VTT, Espoo, Finland*

<sup>6</sup>*Max-Planck-Institut für Plasmaphysik, EURATOM Association, 85748 Garching, Germany*

<sup>7</sup>*EURATOM/CCFE Fusion Association, Culham Science Centre, Abingdon OX14 3DB, Oxon, UK*

<sup>8</sup>*IEF – Plasmaphysik, Forschungszentrum Jülich, TEC, Association EURATOM-FZJ, Germany*

*\* See annex of F. Romanelli et al, “Overview of JET Results”,  
(24th IAEA Fusion Energy Conference, San Diego, USA (2012)).*



## ABSTRACT

When the ITER-like wall was installed in JET, one of the 218 Be inner wall guard limiter tiles had been enriched with  $^{10}\text{Be}$  as a bulk isotopic marker. During the shutdown in 2012–2013, a set of tiles were sampled nondestructively to collect material for Accelerator Mass Spectroscopy (AMS) measurements of  $^{10}\text{Be}$  concentration. The letter shows how the marker experiment was set up, presents first results and compares them to preliminary predictions of marker redistribution, made with the ASCOT numerical code. Finally an outline is shown of what experimental data are likely to become available later and the possibilities for comparison with modeling using the WallDYN, ERO and ASCOT codes are discussed.

## INTRODUCTION

Materials migration between plasma facing surfaces is one of the crucial issues for ITER and other future large fusion devices. The net erosion rate limits the component lifetime at surfaces where erosion dominates, while net deposition in other regions entails undesired fuel trapping by co-deposition and dust production when thick deposits peel off [1]. Deposition at mirrors and windows also creates problems for diagnostics. If more than one plasma facing material is used materials migration causes mixing, which modifies the surface physical properties. The ITER-Like Wall (ILW) program at JET [2] has been implemented to study these and other issues in the case of a wall configuration with beryllium surfaces in the main chamber and tungsten in the divertor. To study how material migrates during plasma operations, one of the inner wall guard limiter (IWGL) tile assemblies in JET was enriched with  $^{10}\text{Be}$ . In samples taken from the wall elements after exposure to plasma the  $^{10}\text{Be}/^{9}\text{Be}$  ratio can be measured using accelerator mass spectrometry (AMS) [3], with sensitivity better than  $10^{-14}$ . To achieve this sensitivity, samples of  $100\mu\text{g}$  Be are sufficient.

Figure 1 shows a sketch of the 10 Be enriched IWGL tile assembly. The three central pieces were irradiated with thermal neutrons in the JEEP-II reactor in Lillestrøm, Norway, and the resulting bulk  $^{10}\text{Be}/^{9}\text{Be}$  isotope ratio due to neutron capture was measured to be  $1.73 \times 10^{-9}$ . Samples of non irradiated Be from the same source as the tile material, as well as a sample containing Be that had been exposed to JET plasma, were analysed and were found to contain  $^{10}\text{Be}/^{9}\text{Be} < 10^{-14}$ .

Background  $^{10}\text{Be}$ , not due to transport in the plasma from the marker tile could *a priori* be expected in the bulk of the Be components as a result of neutron capture of plasma generated neutrons. Capture of 2.45MeV neutrons generated in the DD reactions during the first period of ILW operation can be estimated, taking as upper limit for the average neutron flux at the wall  $5 \times 10^9 \text{ s}^{-1} \text{ cm}^{-2}$ . This is the maximum neutron production rate measured with C wall during an L-mode discharge at 3MW ICRH heating [4]. The total ICRH operation time during the ILW campaign was 2.1h with average power 1.4MW. The neutron capture cross section  $10^{-4}$  barn [5] and the neutron flux integrated over the ICRH time would produce  $^{10}\text{Be}/^{9}\text{Be} < 5 \times 10^{-15}$ , which is below the sensitivity of the AMS method. There could also be contamination anywhere through the sample preparation stages. For this report a practical detection limit for plasma-transported marker is taken as the lowest actually

measured  $^{10}\text{Be}/^{9}\text{Be}$  concentration ratio  $1.2 \times 10^{-13}$ . This includes and probably overestimates all possible sources of background.

The enriched assembly was mounted at the 11th row from the bottom in toroidal section 5Z, at major radius  $R_S = 1.84\text{m}$ , vertical position  $Z_S = 0.4\text{m}$ , as shown by a cross in Figure 2. The tile was exposed to JET plasma throughout the first period of operation with ILW, from August 2011 to July 2012. The total plasma exposure time with plasma current larger than 1MA was 16.1h, 12.5h of which were with X-point formed. After the first period of ILW operations, the IWGL tiles from beam 2X, rendered dark in Figures 2 and 3, were permanently removed for different kinds of analysis, as well as the wing tiles, shown in green in Figure 1. The divertor tiles marked by arrows in Figure 2 were also removed permanently.

In order to extract samples for AMS analysis also from tiles that could not be permanently removed, non destructive sampling was made at 102 different positions on the IWGL tiles, as shown with circular symbols in Figures 3 and 4. The sampling was made abrasively, by pressing circular pieces of sandpaper, mounted on a rotating shaft against the surface, with a predetermined pressure and rotating the paper for a fixed number of turns. The released dust stuck to the sandpaper and could later be extracted for analysis. Through roughness measurements on test Si samples, the sampling depth with this method can be estimated to about  $4\mu\text{m}$ .

To extract sampled material, the abrasive tabs were leached in 4M solution of HCl. 10% of each sample was isolated and processed separately to measure total Be content by the mass spectrometry (ICP-MS) method, using standard protocols for similar specimens [6]. By comparing the total amount of Be in the samples with the sizes of the abraded areas, the average sampled depths could be determined and were typically  $\sim 1\mu\text{m}$ . Liquid samples were precipitated and chemically processed to form solid BeO targets for AMS [7]. Sample preparation and AMS measurements of the  $^{10}\text{Be}/^{9}\text{Be}$  concentration ratio in each sample were performed at the Tandem Laboratory at Uppsala University. The  $^{10}\text{B}$  atomic isobar was separated in the beam line through different energy loss in a thin-foil Ni target. These measures allowed counting  $^{10}\text{Be}$  and  $^{10}\text{B}$  separately and subtraction of the boron contribution from the  $^{10}\text{Be}$  signal. The  $^{10}\text{B}$  background in all cases was found to be negligible. As the area of each sample-point was known, the sampled areal density of  $^{10}\text{Be}$  was determined at every position and the numbers for the first batch of samples to be analysed are shown in Figures 3 and 4. The blue symbols in the figures indicate non destructive samples which have not been analysed yet.

Tile profilometry for the midplane IWGL tile shows a total net erosion of 0.8g at the centre of the tile [8]. For the marker tile this corresponds to  $10^{14}$  eroded  $^{10}\text{Be}$  atoms. From the time integrals of the horizontal spectroscopic Be II signal (527nm) over X-point phases and limiter phases it follows that about 90% of the source sputtering took place in limiter phases. This implies that the gross distribution of  $^{10}\text{Be}$  in the main vessel (excluding divertor) is representative only for limiter operation. Besides the experimental data, Figures 3 and 4 show predictions for the distribution of  $^{10}\text{Be}$  deposition due to direct transport of marker from the primary source by 3D simulations with ASCOT [9]. The simulation is for typical conditions in the limiter phase of a discharge. The measured

areal density of  $10 \text{ Be}$  ranges from  $3 \times 10^6 \text{ cm}^{-2}$  to  $1.2 \times 10^8 \text{ cm}^{-2}$ . If the average areal density of  $^{10}\text{Be}$  at the sides of all 304 IWGL tiles is taken as  $8 \times 10^7 \text{ cm}^{-2}$  (maximum measured deposition on the beam 2X), a total deposition of  $3 \times 10^{12} \text{ }^{10}\text{Be}$  atoms can be inferred for the IWGL. This accounts for only 3% of the estimated  $^{10}\text{Be}$  erosion. Provided that in most places the whole deposited layer was sampled, the conclusion must be that most of the eroded material is deposited elsewhere than in the IWGL.

On beam 2X, in agreement with the simulation, maximum measured  $^{10}\text{Be}$  density is found on the right hand side of tile 14, also below the mid plane average deposition favors left hand side of the limiters. Nevertheless, the measured significant deposition at the mid plane level is not expected from the simulation. On beam 5Z the pattern of local redeposition around the source and leftright asymmetry below the mid plane are in line with the simulation. At the same time, above the mid plane measured marker concentrations are peaking on the left hand side. Measured high local  $^{10}\text{Be}$  concentration around the marker suggests that the ASCOT simulation underestimates the rate of prompt redeposition.

In order to calculate the  $^{10}\text{Be}/^{9}\text{Be}$  concentration ratio in the deposited layers on the IWGL it will be necessary to use information which is still not available regarding the thickness of deposited layers at different positions. Surface profiling at the sides of the IWGL shows significant scatter due to surface roughness and the accuracy was not sufficient to determine thicknesses of the order of  $5\mu\text{m}$  or less [8]. More accurate information about the thickness of the layers is expected from analysis of the marker tiles. AMS analysis will be extended, first to include the missing sampled points shown with blue circles in figures 3 and 4. Samples will then be analysed also from the 2X marker tiles, from the wing tiles on both sides of the  $^{10}\text{Be}$  marker, from divertor tiles in octants 1 and 5, as shown in Figure 2. The  $^{10}\text{Be}$  source tiles remain in place and it will be possible to do AMS analysis on new samples following the next JET shut down, scheduled for 2014.

To allow predictions for Be migration in new conditions, it is necessary to compare the experimental results with modeling. Three different numerical simulation tools are currently available for modeling of wall material migration. The WallDYN [10, 11] code computes the composition change of the first wall as a result of material erosion, subsequent transport, re-deposition and also includes re-erosion. In WallDYN impurity transport in the plasma is described by a re-deposition probability distribution for the material species eroded at each discrete wall element. The discrete distribution functions form a matrix, pre-computed by a suitable impurity transport code such as DIVIMP [12]. The underlying assumption is that the characteristic time scale of impurity transport through the plasma is small compared to the time scale of wall composition changes. This condition is generally met in tokamak discharges except for processes where high wall flux coincides with short time scales, such as for ELM impact. Using a 2D transport code such as DIVIMP further implies toroidal symmetry of the wall, which holds for the divertor and baffle areas. For the main chamber, the assumption of toroidal symmetry is only justified for global calculations, while local processes, such as limiter erosion require full 3D modeling. For X-point plasma conditions the redistribution

matrix [10] suggests that most of the Be eroded at the position of the marker tile will after first flight be deposited at the upper part of the inner divertor and in a poloidal region extending from the upper dump plates to the upper part of the outer poloidal limiters.

The second modeling tool, ASCOT, does not yet include realistic treatment of surface processes, however as a 3D simulation code, it allows to model transport and re-deposition of impurities taking into account the full 3D structure of the JET vessel. Predictions for the redistribution of  $^{10}\text{Be}$  marker in limiter plasma and a representative X-point plasma were made in [9].

The third modelling tool, ERO, is a 3D local plasma impurity transport code, which includes detailed models of plasma/surface interaction and of atomic and molecular processes. The motion of particles in the electric and magnetic fields is modeled, including gyro-motion and the influence of the surface magnetic sheath, which is important e.g. for prompt re-deposition processes. Due to the high computational cost the code is usually applied to limited areas of 3D shaped components facing a restricted plasma volume, up to the dimensions of ITER blanket modules with sizes above 1 m [13]. The code has already been applied to limiter erosion and cavity deposition studies at JET [14, 15]. ERO is ideally suited to model the local erosion and deposition in the region close to the  $^{10}\text{Be}$  source, e.g. at the marker-limiter 'wing' tiles. The density of  $^{10}\text{Be}$  sampling in this local region was enhanced. One can further consider ERO-ASCOT code-code benchmark or a combination, where the latter calculates the global transport from the source erosion simulated in detail by ERO. A main complication in all cases is that the codes take the plasma background as input and demand either additional calculations (SOLPS, EMC3, etc) for the plasma parameters or some 3D mapping interpretation of experimental data from the diagnostics available. Moreover, the  $^{10}\text{Be}$  experimental data are accumulated over extended periods of JET operation and appropriate steps have to be taken for averaging over the erosion and deposition in different conditions. When AMS analysis is completed of the more densely spaced samples from the primary source tile and its adjacent tiles, it will be possible to compare the marker redistribution with detailed ERO simulations. Further on, when AMS results from divertor tiles become available, it will be possible to compare any poloidal and toroidal asymmetries with the predictions from ASCOT for the X-point phase of a typical discharge [9]. Comparisons of the experimental poloidal marker distribution data can then also be made with WallDYN, including re-erosion and migration using the redistribution matrix obtained by ASCOT or ERO or a combination.

In conclusion, a bulk isotopic marker has been employed for the first time to study materials migration in fusion devices. A non destructive method for surface sampling at IWGL in JET has allowed AMS analysis to determine the distribution of marker deposition following the first period of operation with ITER-Like wall. Preliminary results show qualitative agreement with predictions from ASCOT simulations, but more data and modeling will be required to exploit the potential of the experiment.

## ACKNOWLEDGEMENTS

This work was supported by EURATOM and was carried out within the framework of the European Fusion Development Agreement. The views and opinions expressed herein do not necessarily reflect those of the European Commission.

## REFERENCES

- [1]. J. Roth, E. Tsitrone, A. Loarte et. al. *Journal of Nuclear Materials*, **390–391**:1–9, 2009.
- [2]. J. Pamela, G.F. Matthews, V. Philipps et al. *Journal of Nuclear Materials*, **363–391**:1–11, 2007.
- [3]. A. Aldahan and G. Possnert. *Geophysical Research Letters*, **30**:1301, 2003.
- [4]. C. Hellesen et al. *Nuclear Fusion*, **50**:022001, 2010.
- [5]. J. Kopecky. *Atlas of neutron capture cross sections*. International Atomic Energy Agency, 1995.
- [6]. SGAB. *Procedure for the ICP-AES and ICP-MS analyses of sediment*, Internal Report, 1995.
- [7]. A.-M. Berggreen, G. Possnert and A. Aldahan. *Nuclear Instruments and Methods B*, **268**:795–798, 2010.
- [8]. K. Heinola, C.F. Ayres, A. Baron-Wiechec et al. *Physica Scripta*, submitted.
- [9]. J. Miettunen, M. Groth, T. Kurki-Suonio et al. *Journal of Nuclear Materials*, **438**:S612–S615, 2013.
- [10]. K. Schmid, M. Reinelt, K. Krieger. *Journal of Nuclear Materials*, **415**:S284–S288, 2011.
- [11]. K. Schmid. *Journal of Nuclear Materials*, **438**:S484–S487, 2013.
- [12]. P.C. Stangeby and J.D. Elder. *Journal of Nuclear Materials*, **196**:258–263, 1992.
- [13]. D. Borodin, A. Kirschner, S. Carpentier-Chouchana et al. *Physica Scripta*, **T145**:014008, 2011.
- [14]. D. Matveev, A. Kirschner, A. Litnovsky et al. *Plasma Physics and Controlled Fusion*, **52**:075007, 2010.
- [15]. D. Borodin, M.F. Stamp, A. Kirschner et al. *Journal of Nuclear Materials*, **438**:S267–S271, 2013.

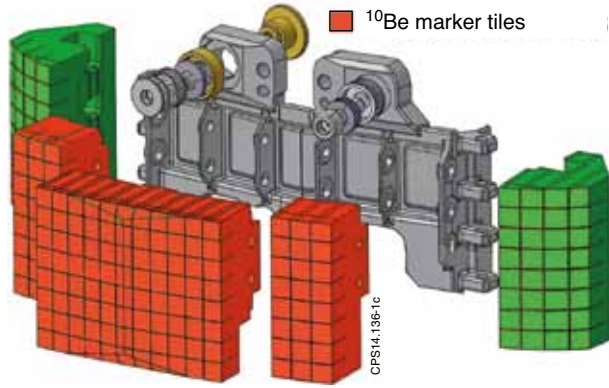


Figure 1:  $^{10}\text{Be}$  isotopic marker tile assembly. The three central tiles are activated to  $^{10}\text{Be}/^{9}\text{Be} = 1.73 \times 10^{-9}$ .

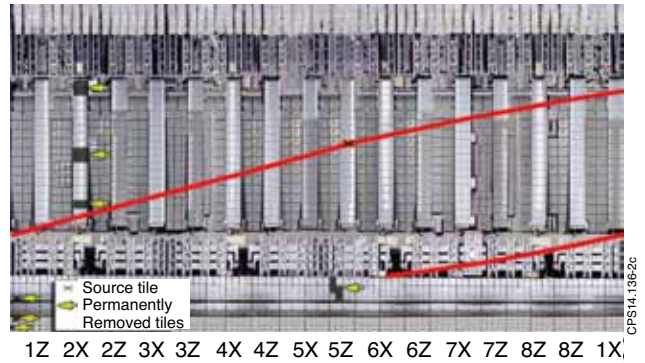


Figure 2: Developed view of JET inner wall with IWGL limiter beams. The  $^{10}\text{Be}$  marker-tile is indicated by a cross in beam 5Z. A magnetic field line corresponding to X-point configuration is plotted, connecting the  $^{10}\text{Be}$  source to the inner divertor target. Arrows indicate positions of permanently removed tiles, which will eventually be available for analysis.

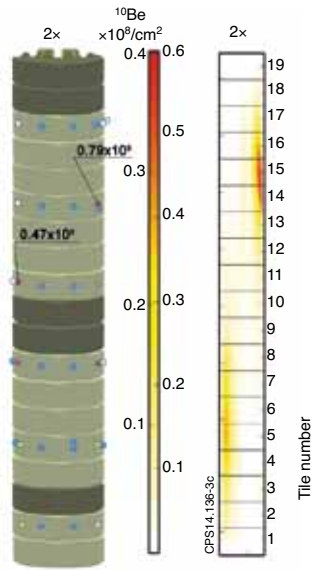


Figure 3: Comparison for IWGL beam 2X of experimentally measured  $^{10}\text{Be}$  marker redistribution (on the left) with ASCOT prediction (on the right). The colored circles in the experimental map mark sampling positions on the tile front surfaces and on the sides. The blue-colored spots denote positions, from where the data will be available later. Two values outside the colour range are indicated with numbers.

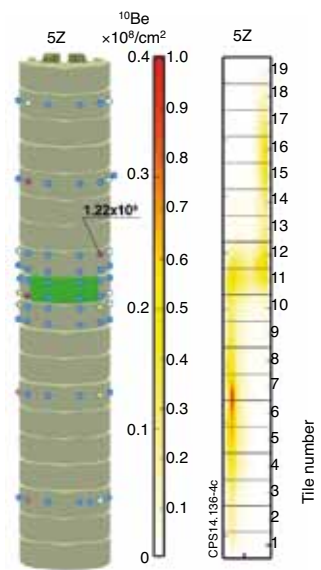


Figure 4: Experimentally measured  $^{10}\text{Be}$  marker redistribution in the IWGL beam 5Z, compared to ASCOT simulation. The colored circles in the map mark sampling positions on the tile front surfaces and on the sides. The blue-colored spots denote positions, from where the data will be available later.  $^{10}\text{Be}$  source tile is shown in green. One value outside the colour range is indicated with number.